Geothermics 64 (2016) 455–465

Geothermics

journal homepage: www.elsevier.com/locate/geothermics

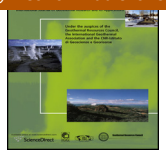

Thermal breakthrough calculations to optimize design of a multiple-stage Enhanced Geothermal System

Tianyu Li, Sogo Shiozawa, Mark W. McClure*

The University of Texas at Austin, Department of Petroleum and Geosystems Engineering, 200 E. Dean Keeton, C0300, Austin, TX 78704, United States

ARTICLE INFO

Article history:
Received 27 October 2015
Received in revised form 15 June 2016
Accepted 22 June 2016
Available online 25 July 2016

Keywords:
EGS
Multiple stages
Thermal breakthrough
Optimization
Horizontal wells

ABSTRACT

We perform an optimization and sensitivity analysis for design of an Enhanced Geothermal System (EGS) with horizontal wells and multiple fracturing stages. The sensitivity analysis includes calculations of thermal breakthrough and the maximum flow rate that can be achieved through the system. The analysis uses idealized reservoir geometry and is intended to investigate the relationship between parameters and provide insight into how to optimize an EGS, not to provide precise predictions of performance. Conventionally, EGS wells have been nearly vertical and stimulated with openhole completion in a single stage. This study investigates a design with two parallel horizontal wells. The first well is drilled and completed with casing, and then stimulated sequentially in stages with cased hole packers rated to high temperature. The second well is drilled through the stimulated region created around the first well and completed openhole. For different combinations of well spacing, lateral length, formation permeability, and number of stages, we calculate the optimal flow rate that maximizes the present value of revenue. The calculations show that stimulating with multiple stages greatly improves economic performance, delays thermal breakthrough, and allows a higher flow rate to be circulated through the system. At low well spacing and low number of stages, it is optimal to circulate fluid more slowly than the maximum possible rate in order to delay thermal breakthrough. With greater well spacing and with more stages, thermal breakthrough is relatively delayed, and it is optimal to circulate at the maximum possible flow rate. Overall, it is optimal to use the lowest well spacing where present value is maximized by circulating at the maximum possible rate. When it is optimal to circulate at the maximum possible rate, present value is sensitive to reservoir transmissivity. When it is optimal to circulate at less than the maximum possible rate, present value is unaffected by reservoir transmissivity. Increasing lateral length beyond 1000 m is only beneficial for designs with relatively low lateral spacing and a large number of stages.

1. Introduction

1.1. Premise

We perform a sensitivity analysis to investigate how various parameters affect the economic performance of an Enhanced Geothermal System (EGS) with horizontal wells and multiple fracturing stages. The calculations use a simplified representation of the reservoir. The objective is to investigate relationships between variables and build insight into optimal EGS design, rather than to provide precise predictions of reservoir and economic performance. The overall results are not dependent on the details of the specific parameters chosen.

A full economic analysis would require consideration of cost, the sale price of electricity, discount rate, reservoir temperature, depth, and other factors. These subjects are outside the scope of this paper. Project revenue in particular cases could be significantly higher or lower, depending on conditions.

Most EGS projects have been performed with a single fracturing stage in nearly vertical wells with openhole completion. A few exceptions are the Schönebeck project, which used packers in several stimulation stages (Zimmermann et al., 2010), AltaRock's Newberry project, which used diverting agents (Petty et al., 2013), and Petratherm's Paralana project, which stimulated from perforated casing in a vertical well (Bendall et al., 2014).

In this study, the performance of an EGS doublet involving flow between parallel horizontal wells is investigated. Multiple stage stimulation is achieved with zonal isolation technology (such as

* Corresponding author.
E-mail addresses: Tianyu.li92@gmail.com (T. Li), mark.w.mccl@gmail.com (M.W. McClure).

http://dx.doi.org/10.1016/j.geothermics.2016.06.015

List of variables

A	Cross-sectional area of the wellbore
BHP_{prod}	Bottomhole pressure of the producer, MPa
BHP_{inj}	Bottomhole pressure of the injector, MPa
c_W	Heat capacity of water, kJ/(kg °C)
c_R	Heat capacity of rock, kJ/(kg °C)
(dp/dz)	Total pressure gradient, Pa/m
$(dp/dz)_F$	Frictional gradient, Pa/m
$(dp/dz)_H$	Hydrostatic gradient, Pa/m
$(dp/dz)_A$	Accelerational gradient, Pa/m
d	Well or pipe diameter, m
E	Electricity production, kW-hr
eff	Efficiency of conversion of thermal energy to electrical, unitless
f	Moody friction factor
H	An arbitrary length used in the Gringarten et al. (1975) solution, m
h	Fracture height, m
i	Discount rate
K_R	Thermal conductivity of rock, J/(m s °C)
L	Spacing between injection and production well, m
N	Number of stages
n	Total years of production
P	Price of electricity, cents/kW-hr
PV	Present value of revenue, $
Q	Volumetric fluid flow rate per fracture per unit height, m^2/s
Q_{prod}	Rate of thermal energy production, J/s
Q_{th}	Rate pf thermal energy production, kW
q	Fluid flow rate, kg/s
Re	Reynolds number, dimensionless
s	Laplace variable, dimensionless
T	Fracture transmissivity (product of permeability and thickness), m^3
T_{RO}	Initial reservoir temperature, °C
T_{WO}	Injection fluid temperature entering the reservoir, °C
$\bar{T}_{WD(z_D,s)}$	Laplace transform of dimensionless fluid outlet temperature
$t_D{}^*$	Dimensionless time variable for laplace transform
t_T	Total years of production, yrs
t	Time, s
t'	Injection time considering the time lag between injection point and arrival at z, s
v	Fluid velocity, m/s
WHP_{inj}	Wellhead pressure of the injector, MPa
WHP_{prod}	Wellhead pressure of the producer, MPa
X_E	Fracture half-spacing, m
X_{ED}	Dimensionless fracture half-spacing
z	Distance, m
z_D	Dimensionless distance
z/v	Time lag between the departure of water from the injection point and the arrival at point z, s
α, β^*	Dimensionless parameters used in the Gringarten et al. (1975) solution
ΔP_{inj}	Pressure drop in the injector, MPa
ΔP_{prod}	Pressure drop in the producer, MPa
ΔP_{res}	Pressure drop in the reservoir, MPa
ΔT	Temperature difference in the surface power plant, °C

List of variables

Δt_j	Duration of time period j, hours
ε	Pipe roughness
θ	Wellbore angle from horizontal, degrees
Λ	A dimensionless parameter used for calculating wellbore friction
μ	Viscosity of fluid, cp or MPa-s
ρ_W	Water density, kg/m^3
ω	Geothermal gradient, °C/m

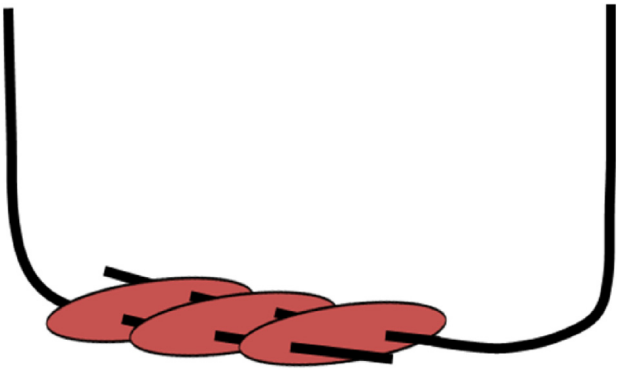

Fig. 1. An EGS doublet of horizontal wells connected by vertical fracture stages (normal or strike-slip faulting regime). The wells are oriented toe to heel in order to encourage equal flow rates between stages. The ellipses represent regions of fracturing, are not intended to be representations of the actual fracturing geometry.

packers). The laterals are oriented so that the stimulated region at each stage forms transverse to the lateral, as shown in Fig. 1. Related designs have been discussed by Gringarten et al. (1975), Cremer et al. (1980), Green and Parker (1992), MacDonald et al. (1992), Jung (2013), Glauser et al. (2013), Shiozawa and McClure (2014), Lowry et al. (2014), Olson et al. (2015), and Doe and McLaren (2016).

Orienting the laterals in opposite directions would help promote uniform flow between the stages (discussed in more detail by Shiozawa and McClure (2014). The wells could be drilled from the same pad (the same surface location), sharing surface facilities such as the mud pit, and with their wellheads located in close proximity. They could be deviated in opposite directions with only modest increase in drilling cost. For example, wells drilled vertically to a depth of 500 m and then deviated at 11.2° from vertical in opposite directions would achieve separation of 1 km at a depth of 3 km, with increase in well length of only 50 m for each well. Additional wells could be drilled from the same pad by using directional drilling to separate the wells laterally. Drilling a large number of wells from the same pad reduces surface footprint and cost (Ogoke et al., 2014).

If drilling horizontally is considered too technically challenging due to high temperature and hard rock, a similar design could be achieved by connecting two wells deviated from vertical. However, in this case, it would not be possible to orient the wells in opposite directions and different stages would be at different temperatures, which would make it more difficult to achieve uniform flow between stages.

Our prior work investigated how using multiple stages increases the maximum achievable flow rate through the system (Shiozawa and McClure, 2014) and delays thermal breakthrough (Li et al., 2014). This paper extends our prior work by using a finite fracture-spacing analytical solution and an improved optimization scheme.

Thermal breakthrough is a complex function of many factors, including the overall flow rate through the system, the number of flowing fractures, the spacing between the laterals, and the spacing between the flowing fractures along the laterals. The ideal lateral spacing and flow rate, depending on the number of stages along the wells, is identified through an optimization process. Present value of revenue is calculated for different numbers of stages, assuming optimal well spacing and flow rate.

We also investigate the sensitivity to the fracture transmissivity (or more precisely, the aggregate transmissivity of the fractures created by stimulation at each stage). The transmissivity of individual fracture is likely to be controlled by in-situ conditions such as lithology, fracture roughness, and stress state (Barton et al., 1985) and may be difficult to control from an engineering point of view. Fracture shear induced by elevated pressure increases the transmissivity of natural fractures in many cases. Proppant would be useful in increasing fracture transmissivity, especially in the near-wellbore region, but would likely be too expensive to use at large scale (for example, by propping the entire fracture formed at each stage).

An important uncertainty is whether newly created hydraulic fractures would be capable of self-propping. The concept of shear stimulation relies on the mismatch of asperities to hold open natural fractures. It is not clear whether asperity mismatch occurs when newly formed fractures close for the first time. New hydraulic fractures have freshly generated roughness and, unlike natural fractures, have not yet been subjected to asperity creep, chemical effects, and other processes that occur over geologic timescales. Newly forming fractures may be sufficiently rough that they are able to self-prop, especially in hard rock such as granite (Jung, 1989). Slickwater fracturing (using little or no proppant) has been very successful for oil and gas productions in shale, and this process depends strongly on newly formed hydraulic fractures retaining transmissivity after closure (King, 2010).

1.2. EGS reservoirs and completion strategy

Since the 1980s, EGS design has been based on the concept of shear stimulation, that an increase in fluid pressure induces slip on preexisting fractures, causing an increase in transmissivity (Pine and Batchelor, 1984; Murphy and Fehler, 1986). The hope has been that this process would stimulate a large, closely spaced, well-connected network of flowing fractures, which would access sufficient volume of rock to enable economically viable production.

Experience has revealed limitations to the conventional EGS design. Well logs have shown that flow tends to localize into a small number of widely spaced fractures at the wellbore and flow rates have consistently been lower than needed (Richards et al., 1994; Ito and Kaieda, 2002; page 533 of Brown et al., 2012; Miyairi and Sorimachi, 1996; Wyborn et al., 2005; Baria et al., 2004; Evans, 2005; Dezayes et al., 2010).

Numerical simulations based on continuum models of the reservoir, such as dual porosity models, tend to be overly optimistic and underestimate the natural tendency for flow localization in fracture networks (Sanyal and Butler, 2005). Discrete fracture network simulations yield more pessimistic (and more realistic) predictions (Doe et al., 2014; Doe and McLaren, 2016).

Field experience has shown that only a few fractures at the well dominate flow. Evans (2005) reviewed wellbore observations at the Soultz EGS project and found that only a small percentage of fractures that were well-oriented to slip according to a Coulomb stress analysis were actually stimulated by injection. Even if a large stimulated network is created, only a small minority of that network may actually be part of a strong hydraulic connection between an injection and production well (Section 2.4.3 from McClure, 2009). When flowing fractures are widely spaced, the heat sweep efficiency is unlikely to be optimal. Rapid thermal breakthrough has been observed at some EGS projects (MacDonald et al., 1992; Tenma et al., 2008).

A second problem has been establishing sufficient hydraulic connection between the injection and production wells. For example, this problem was documented at Fenton Hill (Brown et al., 2012), Rosemanowes (Parker, 1999), and the well GPK4 at Soultz (Genter et al., 2010). In these cases, microseismicity indicated significant regions of stimulation around the wells, but fracture pathways for flow between the wells were limited or weak, resulting in poor hydraulic connection.

Multiple stage fracturing could create reservoirs that can sustain higher circulation rate and access a larger volume of rock. When fluid is pumped into a long wellbore section, fluid tends to flow into the first few fractures that form or that are stimulated at the wellbore (Yoshioka et al., 2015). As a result, stimulation is not evenly distributed along the well. If the stimulation is performed with multiple stages, fractures are forced to form at each stage, creating a much more evenly spaced fracture network. In the oil and gas industry, the use of multiple hydraulic fracture stages has enabled a huge amount of new production from previously uneconomic shale formations (King, 2010).

An objection to the use of multiple stages in EGS has been that openhole packers have not been proven to work reliably at high temperature. Olson et al. (2015) found that openhole packers rated to geothermal temperatures are now available off-the-shelf, but acknowledged that this technology is relatively less proven. As reviewed by Shiozawa and McClure (2014), cased hole packers rated to geothermal temperatures are available off-the-shelf from oil and gas service companies and are more likely to be reliable because they avoid the problem of wellbore roughness and non-circular geometry.

EGS projects have nearly always been completed in openhole, both to save cost and to maximize contact with natural fractures (because the goal has been to stimulate natural fractures). However, it is possible to perform stimulation out of perforated, cased wells. Bendall et al. (2014) reported on a well that was recently stimulated in granite at 3.68 km depth out of a perforated, cased well at 190 °C. A successful casing perforation operation in a geothermal well in the Salavatli geothermal field was discussed by Serpen and Aksoy (2015). Yoshioka et al. (2015) reported greatly improved stimulation performance after zonal isolation was used for a fracturing treatment performed in the Salak field.

Glauser et al. (2013) investigated whether completing EGS wells with perforated casing would cause excessive near-wellbore pressure drop. Pressure drop during flow through perforations scales with the square of flow rate and the fourth power of diameter (Willingham et al., 1993). Furthermore, the initiation of hydraulic fractures from perforations can cause near-wellbore fracture network complexity. Glauser et al. (2013) concluded that flow rate reduction due to flow through perforations can be minimized and managed with appropriate engineering.

Perforation pressure drop may be advantageous for EGS. In hydraulic fracture design, perforations are sometimes intentionally created with a relatively small diameter, to increase perforation pressure drop and encourage more uniform flow out of the perforations, a strategy called "limited entry completion" (Lecampion et al., 2015). For good heat sweep efficiency during long-term circulation, it would desirable for flow to be as uniform as possible across the stages. Therefore, perforations could be designed to improve sweep efficiency and prevent thermal short circuiting.

If a short-circuit develops, it could be mitigated by pumping a clogging material into the section of the wellbore that contains the short-circuit. This type of wellbore intervention requires zonal isolation that would be easier in a cased wellbore.

Shear stimulation of natural fractures is not necessarily the ideal strategy for creating an EGS reservoir. An optimal EGS design would be highly repeatable, but shear stimulation is dependent on the local details of the natural fracture network. It may be advantageous in EGS to attempt conventional hydraulic fracturing, in which fluid is pumped out of the well with the intention of creating and propagating newly forming fractures. For a variety of reasons, investigators have predominantly believed that the primary mechanism of stimulation in EGS is shear stimulation (summarized by McClure and Horne, 2014). In contrast, McClure and Horne (2014) argued that new fractures probably have formed and propagated at most historical EGS projects.

There are several operational decisions that could be made to increase the probability of new hydraulic fractures forming. If injection is performed into a perforated, cased hole, new fractures would be more likely to form than during pumping into openhole because the perforations would be unlikely to intersect natural fractures (unless the perforations were intentionally located to intersect them, as discussed by Becker et al., 2016). Another strategy would be pumping of a more viscous fluid, which would be more likely to create "simple" fracture geometry, something more similar to a single planar fracture, rather than a complex fracture network, involving a more volumetric region of fracturing (Cipolla et al., 2008).

A "simple" fracture at each stage might appear to be undesirable because it would not create a large number of flowing fractures, which is required for a quality EGS reservoir. But the use of multiple fracturing stages would naturally create a large number of flowing features. Thus we propose to create a large number of relatively "simple" fractures using multiple stages, rather than attempting to create a massive fracture network from a single stage.

Regardless of stimulation mechanism, either new fractures or shear stimulation of natural fractures, it is clear that having additional fracture stages would permit the formation of additional flow pathways by preventing injection fluid from diverting into a small number of features at the wellbore during stimulation.

Drilling deviated wellbores and using multiple fracturing stages would increase cost. A review of the incremental cost of these strategies is outside the scope of this paper. However, our sensitivity analysis indicates that these strategies could increase revenue by an order of magnitude. It is unlikely that the drilling and stimulation cost would increase sufficiently to offset such a large increase in revenue. Geothermal horizontal well drilling cost estimates developed by Baker Hughes found that drilling a horizontal well with 914 m horizontal offset at a depth of 3048 m would increase well cost from $6.7 million to $9.2 million, compared to a vertical well at the same depth (Table 3 from Lowry et al., 2014). Stimulation costs are only a small overall percentage of the total project cost in an EGS project (Sanyal, 2010).

2. Materials and methods

Five elements in EGS design are: (1) flow rate, (2) the number of fracture stages, (3) the spacing between the wells, (4) total well length, and (5) reservoir transmissivity. In our sensitivity analysis, these factors are varied to maximize the present value (PV) of revenue of an EGS doublet. For each combination of parameters, an analytical expression is used to calculate the temperature of produced water over time. These values are converted into thermal production electricity production, and present value.

2.1. Flow rate calculation

For each combination of parameters, the maximum flow rate possible through the system is calculated. The calculations include pressure gradient in the injection well, the reservoir, and the production well. The geometry of the vertical section of the wells is chosen to be consistent with the wells GPK2 and GPK3 at the Soultz EGS project (details given in Table 2; based on Tischner et al., 2006). A horizontal lateral added in our calculations, which was not present in the Soultz wells. The wells are oriented toe-to-heel, as shown in Fig. 1. For simplicity, the temperatures in the injector well, production well, and the reservoir are assumed to be constant for the flow rate calculation (but different in each of the three). This assumption is made only for the calculation of maximum possible flow rate, and affects the solution only because fluid viscosity and density are functions of temperature. This assumption is not made in the thermal drawdown calculations, which use constant circulation rate (as described in Section 2.2).

Table 1
Properties used in the flow rate calculations. In Section 3.4, calculations are performed with alternative values of transmissivity.

Properties	Injector	Reservoir	Producer
Temperature (°C)	60	190	180
Fluid density (kg/m^3)	983.2	873.9	885
Fluid viscosity (cp)	0.466	0.142	0.151
Transmissivity (m^3)		3.07E-13	

The wellhead pressure of the injector, WHP_{inj}, and the wellhead pressure of the producer, WHP_{prod} are specified to be 4 MPa and 0.75 MPa, respectively (following the Soultz circulation test described by Tischner et al., 2006). Circulation is also driven by the difference in density between the fluid in the injection well and the production well. Flow rate could be increased by using a higher injection pressure, but high injection pressure may lead to excessive fluid loss, and so would need to be carefully selected. Flow rate could also be increased by pumping the production well, but this would involve additional cost and parasitic power loss. In practice, decisions about injection pressure and pumping would be made based on site-specific factors.

For the calculation of pressure drop in the wells, it is assumed that all fluid enters or exits the wellbores at a single location, the middle of each of the two laterals (even though the system actually involves wells with multiple stages). This simplification is made solely for the purposes of calculating the frictional pressure drop in the wellbore. This assumption is necessary because frictional pressure drop is a nonlinear function of flow rate. A more detailed calculation would need to account for the decrease in flow velocity after the fluid inflow/outflow at each stage.

The system is modeled as four nodes connected in series: WHP_{inj}, BHP_{inj}, BHP_{prod}, and WHP_{prod}, where BHP_{inj} and BHP_{prod} are the bottomhole pressure of the injector and the producer wells, respectively. Wellbore pressure drop calculations are used to calculate ΔP_{inj}, equal to $WHP_{inj} - BHP_{inj}$, and ΔP_{prod}, equal to $WHP_{prod} - BHP_{prod}$.

Darcy's law is used to calculate ΔP_{res}, equal to $BHP_{inj} - BHP_{prod}$. The transmissivity of the reservoir is defined as the product of the reservoir thickness and permeability and can be applied directly in Darcy's law (Eq. (8)). This definition is often applied to describe flow through fractures, when it is equal to the product of fracture permeability and aperture. If there are multiple fractures flowing in parallel, then the overall transmissivity is the summation of the transmissivity of each individual fracture. All fluid in the system is assumed to be single phase liquid water.

For a given value of reservoir transmissivity, the flow rate through the system is calculated by numerically solving the following nonlinear equation, with flow rate, q, as the unknown:

$$WHP_{prod} = WHP_{inj} + \Delta P_{inj}(q) + \Delta P_{res}(q) + \Delta P_{prod}(q), \quad (1)$$

The equation is solved with an iterative line search method implemented in a Matlab script.

2.1.1. Pressure change calculation in the injection well and the production well

This section explains how $\Delta P_{inj}(q)$ and $\Delta P_{prod}(q)$ are calculated. The total pressure gradient (dp/dz) can be calculated as the sum of the frictional gradient $(dp/dz)_F$, the hydrostatic gradient $(dp/dz)_H$, and the accelerational gradient $(dp/dz)_A$ (Hasan and Kabir, 2002) and is given by:

$$(dp/dz) = (dp/dz)_F + (dp/dz)_H + (dp/dz)_A. \quad (2)$$

For both the injector and production wells, these terms are integrated over the length of the well. The hydrostatic and the acceleration gradients are represented by:

$$(dp/dz)_H = -g\rho_W \sin(\theta), \quad (3)$$

$$(dp/dz)_A = -(q/A)\, dv/dt = -\rho v dv/dz, \quad (4)$$

where ρ_W is the density of fluid, θ is the wellbore angle from horizontal line, q is the mass flow rate, A is cross-sectional area of casing, and v is the fluid velocity.The frictional pressure gradient is:

$$(dp/dz)_F = -fv^2\rho_W/(2d) = -f\rho_W\left(\frac{q}{\rho_W A}\right)^2/(2d), \quad (5)$$

where d is well or pipe diameter and f is the Moody friction factor, which depends on the turbulence of the fluid and also on the pipe roughness.

Chen (1979) proposed the following equation to calculate the Moody friction factor:

$$f = \frac{1}{\left[2\log\left(\frac{\varepsilon/d}{3.7065} - \frac{5.0452}{Re}\log\Lambda\right)\right]^2}, \quad (6)$$

where ε is pipe roughness, and Λ is the dimensionless parameter given by:

$$\Lambda = \frac{(\varepsilon/d)^{1.1098}}{2.8257} + \left(\frac{7.149}{Re}\right)^{0.8981}, \quad (7)$$

where Re is the Reynold's number.

Fluid properties are given in Table 1. The temperature in the injection well is assumed to be 60 °C, and the temperature in the production well is assumed to be 180 °C, both values based roughly on the Soultz reservoir. The surface roughness of casing is assumed to be 150 μm, as estimated for the wellbore casing of GPK2 at Soultz by Mégel et al. (2005) based on measurements of the wellhead and bottomhole pressure during injection.

Table 2 describes the geometry of the injection and production wells (based on the Soultz wells GPK2 and GPK3) including depth, casing diameter and inclination (Tischner et al., 2006). Table 2 contains the extended laterals on the horizontal wells (which were not present in GPK2 and GPK3). The total lateral length is fixed at a particular value (either 1 km or 2 km), and so the distance between the stages (used in the thermal drawdown calculations) is decreased as the number of stages increases. The horizontal part of the injection well is assumed to be completed with casing and perforations (cased hole completion). The horizontal lateral of the production well is assumed to be openhole. The roughness of the wellbore in the openhole is assumed to be 2000 μm. Pressure drop in the perforations is not included in the calculation.

Considering the flow geometry shown in Fig. 1, each molecule of water will pass through the same length of wellbore lateral as it passes through the system (regardless of which stage it flowed through), and that length is equal to half of the total length of both the laterals.

2.1.2. Pressure change calculation in the reservoir

The pressure change through the reservoir is calculated from Darcy's law, assuming steady-state and linear flow through a fracture with height h and transmissivity T:

$$\Delta P_{res} = \frac{q\mu L}{Th\rho_W}, \quad (8)$$

where ΔP_{res} is equal to $BHP_{inj} - BHP_{prod}$, μ is the fluid viscosity, and L is the distance between the injection and production laterals (the well spacing).

The Soultz project is used to make a baseline estimate for the transmissivity of an EGS reservoir. During the 2005 circulation test at Soultz, a 12 kg/s flow rate was sustained between GPK2 and GPK3. The openhole section of the wells was roughly 500 m and the well separation was roughly 600 m. Using those parameters, and using the reservoir and wellbore properties given in Table 1 and Table 2 (which are based on the Soultz circulation test), the overall reservoir transmissivity can be estimated from Darcy's law to be 3.07×10^{-13} m^3 (details provided in the Appendix of Wang et al., 2009).

Spinner logs at Soultz indicated that typically the majority of flow localized into a single fault zone, though in GPK4, spinner logs indicated the formation of an axial hydraulic fracture (Tischner et al., 2007). The reservoir at Soultz benefitted from the presence of very large, thick porous fault zones (Evans, 2005), which are not always present in EGS reservoirs. Therefore, it might be argued that it is overoptimistic to use the aggregate reservoir performance of Soultz as a base case. In Section 3.4, the reservoir transmissivity is varied in order to estimate its effect on economic performance and system design.

The exact nature and geometry of the fracture network at Soultz (or the network created in our hypothetical EGS system) is not important for the calculation. We use a single number, reservoir transmissivity, to account for the aggregate flow capacity of the created fracture network, whether it was a single, planar hydraulic fracture, a dense network of stimulated natural fracture, a large, thick, shear stimulated fault zone, or a network of both new and preexisting fractures.

In this hypothetical EGS doublet, h is assumed to be 200 m. The wellbore spacing L is a design parameter. When there are multiple stages, we assume that flow is evenly distributed between each stage. Therefore, the flow rate per stage is q/N, where N is the number of stages. Equivalently, we can say that the total system transmissivity is equal to $T \times N$. This can be derived from Darcy's law for flow in parallel through multiple independent zones of porous media. This calculation is analogous to the calculation that the electrical conductance of a parallel circuit is equal to the summation of the individual conductances (or equivalently, that the total resistance is equal to the harmonic average of the individual resistances). Table 1 shows the fluid properties used in the calculations.

It is optimistic to assume that fluid will be evenly distributed between each stage. However, as discussed in Section 1.2, perforation pressure drop could be exploited to more evenly distribute flow across each stage. Also, our model makes the rather pessimistic assumption that flow is localized to only a single fracture at each stage. In reality, flow may distribute across multiple fractures, improving heat sweep efficiency. These details could be addressed in a more detailed optimization study, but are outside the scope of the present work.

2.2. Heat extraction from the fractured rock

The analytical solution developed by Gringarten et al. (1975) is used to calculate the fluid temperature at the producer as a function of time. The solution assumes a series of parallel planar fractures in

Table 2
Geometry and well head pressures of the injection well and production well. The wells are assumed to have a sharp kink in geometry between the primarily vertical section and the lateral section.

Wellbore	Measured depth (m)	Pipe diameter (in)	Wellbore angle from horizontal (°)	Wellhead pressure (MPa)
Vertical section of the	0–2373		83.7	
injection well (based	2373–3449		70.9	
on GPK2)	3449–4282		70.9	
	4282–4550		90	
	4550–4610	9 3/8	75	
Lateral section of the injection well (cased hole)	4610 – [5610 or 6610]	9 3/8	0	4
Vertical section of the production well (based on GPK3)	0–534	13 5/8	90	
	534–4084			
	4084–4638	7	79.2	
Lateral section of the production well (open hole)	4638 – [5638 or 6638]	8 1/2	0	0.75

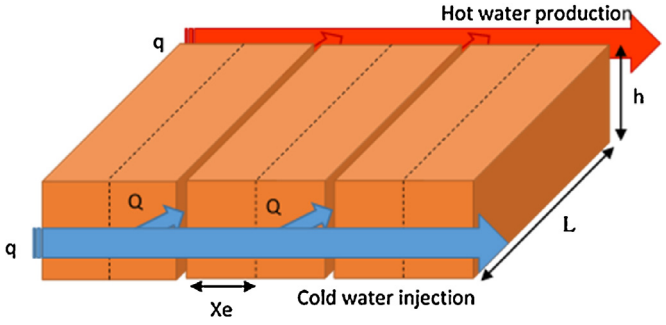

Fig. 2. Schematic of the Gringarten et al. (1975) analytical solution.

the reservoir with height of h and length of L. The distance between the fractures is twice the fracture half-spacing, X_e, and the total number of fractures (equal to the number of stages) is N. Water from the injection well flows through the fractures, heats as it flow through the formation, and enters the production well. Fig. 2 shows a schematic of the problem setup.

The full solution of Gringarten et al. (1975) is implemented to calculate thermal drawdown for parallel fractures of finite spacing (Eq. (9)). To perform the calculation, we use a code that was written by Doe et al. (2014). The solution assumes a periodic boundary condition (infinite series of fractures), neglects heat transfer into the system from above and below, and requires a numerical inverse Laplace transform with respect to dimensionless time t_D^*:

$$\bar{T}_{WD(z_D,s)} = \left(\frac{1}{s}\right)\left[1+\left(\frac{\beta^*}{s^{\frac{1}{2}}\tanh\left[\frac{x_{ED}-1}{\alpha}\right]s^{\frac{1}{2}}}\right)\right]\exp\left(-z_D s^{\frac{1}{2}}\tanh\left(\frac{X_{ED}-1}{\alpha}\right)s^{\frac{1}{2}}\right), \quad (9)$$
$$+\frac{\beta^* z_D}{s} - \frac{\beta^*}{s^{3/2}\tanh\left[\frac{x_{ED}-1}{\alpha}\right]s^{1/2}}$$

where:

$$\beta* = \omega H/(T_{RO}-T_{WO}), \quad (10)$$

$$\alpha = 2K_R H/\rho_W c_W Q b, \quad (11)$$

$$z_D = z/H, \quad (12)$$

$$t_D* = [(\rho_W c_W)^2/4K_R\rho_R c_R]/(Q/H)^2 t', \quad (13)$$

$$X_{ED} = (\rho_W c_W/K_R)(Q/z)x_E, \quad (14)$$

$$t' = t - z/v, \quad (15)$$

$$Q = q/(Nh\rho_W). \quad (16)$$

Doe and McLaren (2016) compared the Gringarten et al. (1975) solution to thermal drawdown data from the Rosemanowes EGS project, and found that it did a good job of matching the data. Therefore, while it is clearly simplified, we believe it reasonably provides a first-order prediction of production temperature.

Table 3 provides the values used in the thermal drawdown calculations. z/v is the time lag between the departure of water from the injection point and the arrival at point z. For prediction $t' \sim t$ of long-term thermal drawdown, $t \gg z/v$, and so

The fracture height is set to be 200 m. At Soultz, the microseismic cloud extended vertically nearly 1500 m, from 4000 m to 5500 m depth (Tischner et al., 2007). However, for this study, we chose to use a more conservative value of 200 m, based on the assumption that the extent of stimulation in each stage will be smaller than the stimulations at Soultz, and the entire vertical section of the stimulated region will not sweep uniformly.

2.3. Conversion to electricity production

The thermal energy production rate in time period j is calculated as:

$$Q_{th,j} = qc_W \Delta T_j, \quad (17)$$

where c_W is the heat capacity of water, and ΔT_j is the difference between the production temperature and the power plant outlet temperature (assumed to be 60 °C). Total electricity production in a particular time period j is calculated as:

$$E(j) = Q_{th,j}\Delta t_j eff, \quad (18)$$

where Δt_j is the duration of time period j. The energy conversion efficiency, eff, is assumed to be 12.63% (Eq. (7)).1 from Tester, 2006). Higher efficiencies may be possible in practice with newer technologies and higher temperatures.

2.4. Present value (PV) calculation

The PV of the project is calculated as:

$$PV = \sum_{j=1}^{j=n} \frac{E(j)P}{(1+i)^j}, \quad (19)$$

Table 3
Parameters used in heat extraction calculations.

Parameter	Symbol	Value	Units	Comments
Fracture height	h	200	m	–
Initial formation temperature	T_{RO}	190	°C	–
Injection temperature	T_{WO}	60	°C	–
Thermal conductivity of rock	K_R	3.01248	J/(s m °C)	For granite
Heat capacity of rock	c_R	1.0	kJ/(kg<remove-image>)	–
Heat capacity of water	c_W	4.420	kJ/(kg<remove-image>)	–
Rock density	ρ_R	2500	kg/m^3	–
Water density in the reservoir	ρ_W	873.9	kg/m^3	–
Arbitrary length	H	5	M	–

where i is the annual discount rate, P is the price of electricity, and n is the number of time periods (equal to either 30 years or the number of years until production temperature reaches 150 °C, whichever is smaller). When the produced fluid reaches 150 °C, it is assumed that the power plant is shut down and no further energy is produced. We assume the price of electricity to be 5 cents per kW-hr and the discount rate to be 16% per year.

The assumed price of electricity is in the range of typical wholesale electricity prices in the United States (Shear, 2015). The discount rate is fairly high, but reflects the risk premium that would likely be placed on financing of an EGS investment. For example, Mines and Nathwani (2013) estimated that a discount rate of 30% per year would be applied during early development of an EGS field, 15% per year during field development, and 7% per year for power plant construction and operations. There is large geographic variability in electricity prices across the US and worldwide, and in many places, government support is available to provide assistance with both electricity price and financing. Therefore, much more favorable economic parameters will be possible in some cases.

2.5. Present value (PV) optimization

We calculate the present value of revenue (PV) for different combinations of parameters. For each combination of well spacing and well length, the optimal flow rate is found using the built-in Matlab optimization function "fmincon."

Several separate optimization calculations are performed. For the first set of calculations, transmissivity is set to the baseline value of 3.07×10^{-13} m^3 per stage and the lateral length is set to 1000 m. A range of values for number of stages are tested. For each value of number of stages, the maximum possible circulation rate is calculated. Then the optimal circulation rate is determined (which may or may not be equal to the maximum possible flow rate), and the present value of revenue is calculated. The process is performed for different lateral lengths (1000 m and 2000 m) and different values of well spacing (200 m, 400 m, 600 m, and 800 m).

3. Results and discussion

3.1. Maximum flow rate

Fig. 3 shows the maximum possible circulation rate as a function of the number of stages and well spacing, assuming the well lateral length is 1000 m.

The maximum rate is limited by pressure drop in the wellbore and in the reservoir. At low numbers of stages, the pressure drop occurs almost entirely in the reservoir. The pressure drop in the reservoir scales directly with spacing (Eq. (8)), and so greater rates are possible with lower spacing. The pressure drop in the reservoir scales inversely with the number of stages, and so as the number of stages grows larger, the proportion of pressure drop occurring in the reservoir decreases. As a result, flow rate through the systems grows roughly linearly with number of stages when there are fewer

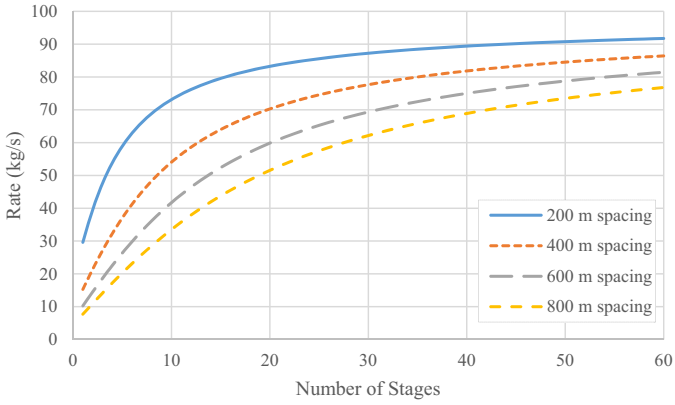

Fig. 3. The maximum possible circulation rate for different values of spacing and number of stages, 1000 m lateral.

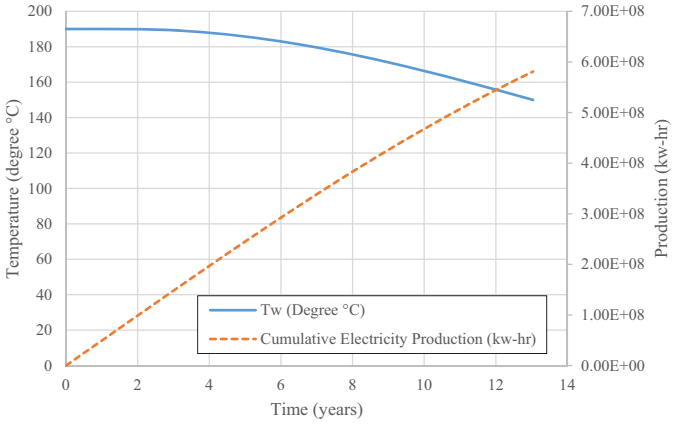

Fig. 4. Example of a temperature and cumulative production profile.

stages and greater well separation (when wellbore pressure drop is negligible). As the overall pressure drop in the reservoir decreases, the marginal effect of adding stages decreases as the pressure drop in the wellbore limits further increases in rate.

This result indicates that wellbore diameter is an important parameter for very high quality reservoirs. Frictional pressure drop scales with the fourth power of diameter. In design of an EGS, wellbore diameter would need to be carefully optimized, considering its effect on both cost and revenue.

3.2. Temperature and cumulative electricity production profile

Fig. 4 shows an example of a plot of temperature and cumulative electricity production versus time. The figure shows the result from the particular case with 60 stages, 400 m well spacing, and 1000 m well lateral length, with circulation at the maximum possible rate of 85 kg/s (Fig. 3). The plot ends after about 13 years because at

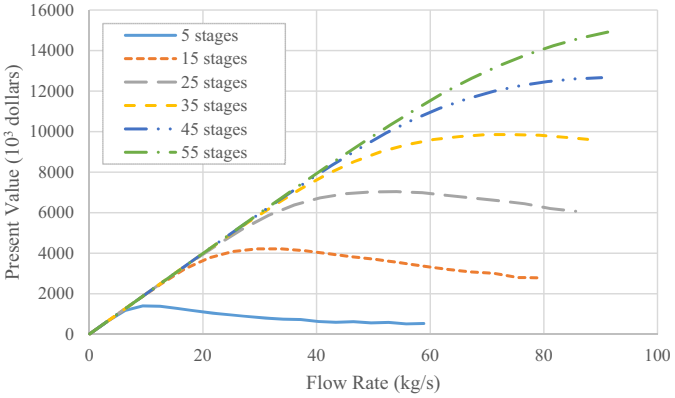

Fig. 5. Present value versus flow rate for 200 m well spacing, 1000 m lateral, and 5–55 stages.

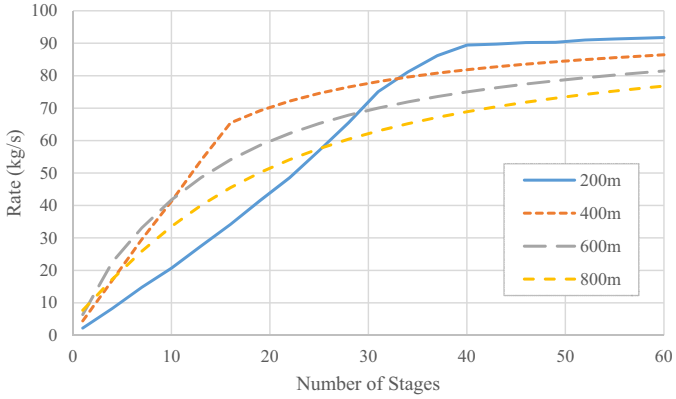

Fig. 6. The circulation rate to achieve optimal present value for different numbers of stages, 1000 m lateral.

this point the temperature has reached 150 °C and so production is terminated. In this case, thermal drawdown begins after only a few years, but progresses slowly enough that the cutoff temperature of 150 °C is not reached until nearly 13 years of production.

In this example, 13 years of production may seem to be insufficient. But when discount rate is considered, it becomes apparent that the economically optimal lifespan of an EGS doublet may be in the vicinity of 10–15 years. At the relatively high, risk-weighted discount rate of 16% per year, revenue 13 years in the future is worth only 10% of revenue in the present. Sanyal (2010) considered optimization of EGS design, and recommended limiting circulation rate in order to maximize project lifespan. But Sanyal (2010) assumed a discount rate of zero, an assumption that would not be made by a profit-driven source of project financing (Mines and Nathwani, 2013). Power purchase agreements and power plant lifespans are typically much longer than 13 years. Therefore, the optimal plan would likely be to thermally draw down an initial batch of wells in roughly 10–15 years and then drill makeup wells once they have begun to experience cooling. Increasing circulation rate lowers heat sweep efficiency (Doe et al., 2014), and so the overall optimal rate would need to be determined through a detailed optimization process. Over several decades, thermally depleted regions would reheat due to natural convection and conduction, enabling the long-term sustainability of the resource (Fox et al., 2013).

3.3. *Optimal present value and flow rate for different well spacing*

Fig. 5 shows present value of revenue as a function of circulation rate for 200 m well spacing and for 5, 15, 25, 35, 45 and 55 stages. The curves end at the maximum rate possible for that number of stages. For wells with 5, 15, 25 and 35 stages, the optimal rate is less than the maximum possible rate. If circulation rate is too high, thermal breakthrough is too rapid and present value is not maximized. If circulation rate is too low, thermal breakthrough is avoided, but the productive capacity of the reservoir is not maximized. For wells with 45 and 55 stages, the optimal rate is equal to the maximum rate, and the curves monotonically increase.

Fig. 6 shows the present value-optimizing circulation rate as a function of the number of stages and for several values of well spacing. For cases with smaller number of stages and shorter well spacing, the optimal rate is limited by the potential for thermal breakthrough. Fluid is circulated more slowly than is possible through the system. For example, Fig. 3 and Fig. 6 show that for the case with one stage and 200 m spacing, the maximum circulation rate is around 30 kg/s, but the optimal rate is around 2 kg/s. This is not an optimal spacing because if the wells were spaced further apart, thermal breakthrough would be further delayed, and

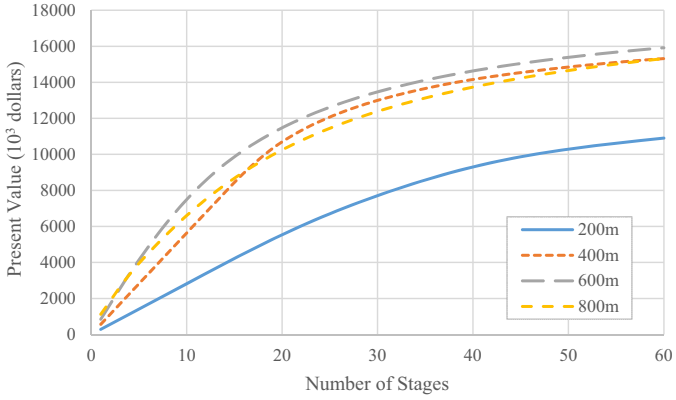

Fig. 7. Optimal present value for different numbers of stages and different well spacing, 1000 m lateral.

present value would be increased. Increasing the spacing lowers the maximum circulation rate, but this does not have a negative effect on the optimal present value of revenue because the optimal rate is lower than the maximum rate. Increasing the number of stages increases present value (Fig. 7) because it spreads flow over a greater number of fractures and improves the heat sweep efficiency, enabling a higher circulation rate to be used without premature thermal breakthrough.

In cases with a greater number of stages and greater well spacing, it is optimal to circulate fluid at the maximum possible rate. In these cases, increasing the number of stages increases present value (Fig. 7) primarily because it increases the maximum possible flow rate through the system. In this case, increasing the well spacing further would not be advantageous because this would lower the total flow rate without having a sufficiently beneficial effect in delaying thermal drawdown. The optimal design occurs at the minimum well spacing where it is optimal to circulate fluid at the maximum possible rate.

Fig. 7 shows present value (assuming circulation at the optimal rate) as a function of well spacing and number of stages. The highest present value is reached with the 600 m well spacing. It shows the present value is controlled by both the maximum flow rate and thermal breakthrough effect. For fewer than 17 stages, 800 m well spacing has a higher present value than the 400 m well spacing because the wells with 400 m well spacing are limited by the thermal breakthrough. With 17 or more stages, the 400 m well spacing has a higher present value than the 800 m spacing. This occurs because with a larger number of stages, present value is con-

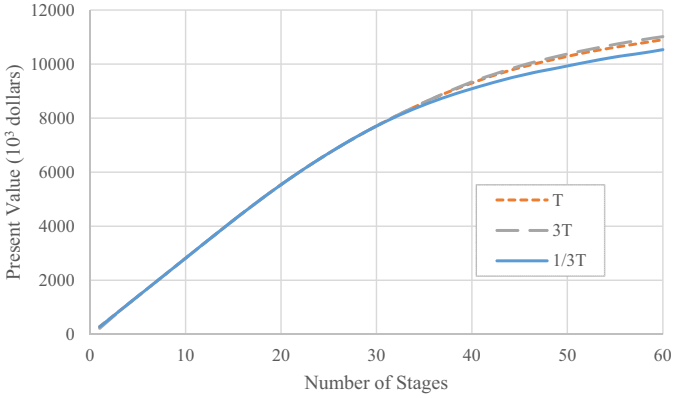

Fig. 8. The optimal present value for wells with 200 m spacing and different transmissivities, 1000 m lateral.

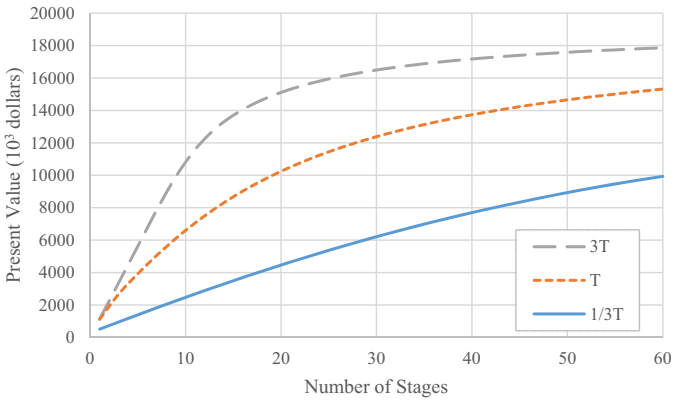

Fig. 9. The optimal present value for wells with 800 m spacing and different transmissivities, 1000 m lateral.

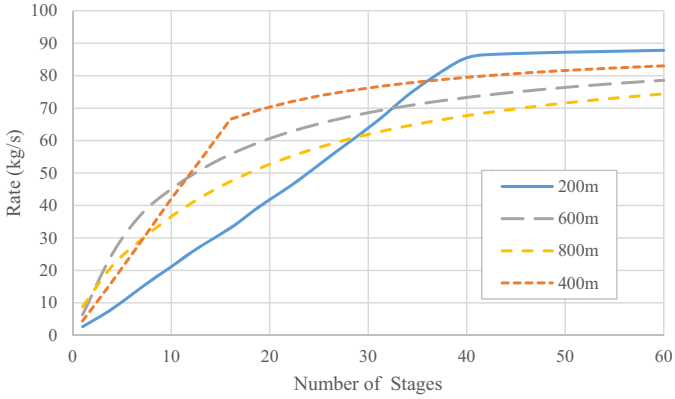

Fig. 10. Optimal rates to achieve maximum present value for wells with a 2000 m lateral.

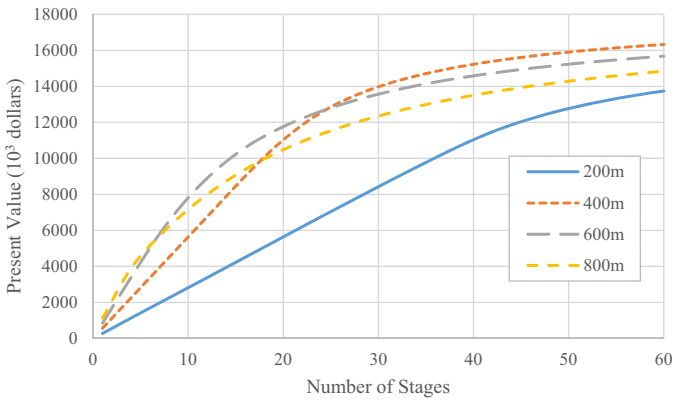

Fig. 11. Optimal present value for each number of stages, 2000 m lateral.

trolled by maximum flow rate, rather than thermal breakthrough, and lowering the spacing allows rate to be increased.

Even though these calculations seem to suggest that 200 m spacing is not ideal, it may be unrealistic to assume that fracture transmissivity is not a function of well spacing. With greater well spacing, it will be more difficult to propagate hydraulic fractures far enough and with sufficient conductivity to achieve good hydraulic connection. Therefore, in practice, a design with 200 m spacing might be chosen in order to ensure good connection between the injector and producer. With lower spacing, it is even more important to use a large number of stages in order to maximize heat sweep efficiency.

3.4. Optimal present value for different transmissivity settings

Figs. 8 and 9 show the present value at optimal circulation rate versus number of stages for three different values of reservoir transmissivity and well spacing of 200 m and 800 m, respectively. At low well spacing and low numbers of stages, the present value is insensitive to reservoir transmissivity. This occurs because it is optimal to circulate fluid at much lower than the maximum rate. At 800 m spacing, it is optimal to circulate at the maximum possible rate. As a result, the present value is highly sensitive to reservoir transmissivity.

3.5. Optimal present value for a longer well lateral length

Figs. 10 and 11 show the optimal rate versus number of stages and optimal present value versus number of stages for four values of well spacing, calculated with a total lateral length of 2000 m. These figures can be compared to Figs. 6 and 7, which assume the well lateral length is 1000 m. Increasing the lateral length delays thermal breakthrough by allowing the fracturing stages to be spaced further apart. The effect of increasing lateral length is greatest for wells with small well spacing and large number of stages. Increasing the lateral length also increases the distance fluid must travel through the well, increasing wellbore pressure drop and decreasing the maximum possible flow rate.

Depending on the number of stages, the optimal spacing may be 800, 600, or 400 m. With more stages, a greater volume of rock is accessed, and so the wells can be placed closer together without risking early thermal breakthrough. When the wells are placed closer together, higher circulation rates are possible.

For well spacing of 400 m or more, the present value of the system is only modestly increased by increasing the lateral length from 1000 m to 2000 m. This indicates that a lateral length of 1000 m accesses sufficient rock volume for economic production at wells with relatively large well spacing.

Fig. 12 indicates that for wells with lower well spacing (200 m), the present value can be increased significantly by increasing lateral length, but only if a large number of stages is used. If a smaller number of stages is used with the longer lateral, the distance between the stages is too great, and there is poor heat sweep efficiency.

4. Conclusions

Fig. 7 shows that the present value of revenue increases greatly as the number of stages increases. Performing stimulation with multiple stages creates a larger number of flow paths, enabling higher flow rate and access to a larger volume of rock. As reviewed

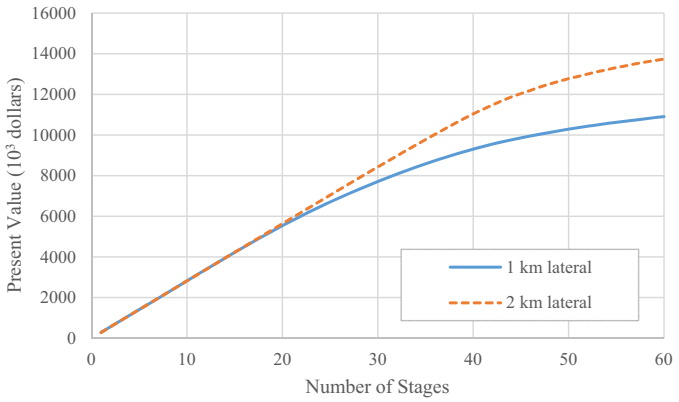

Fig. 12. Comparison of optimal present values between wells with different lateral length (for 200 m spacing).

in Section 1.2, conventional, single stage EGS designs have been able to stimulate a limited number of flowing fracture pathways. Therefore, conventional EGS designs can be considered equivalent to the cases shown in Fig. 7 with around 1–6 stages (indicating 1–6 major flowing pathways).

Full economic evaluation of the horizontal well, multiple stage design would require consideration of cost, which was not included in this study. However, adding a horizontal lateral and performing multiple stimulation stages would result in only a fractional increase in the total cost of the project (Section 1.2). Our study finds that multiple stages can increase revenue by more than an order of magnitude (Fig. 7), which would almost certainly offset the additional cost.

The optimal wellbore spacing occurs at the lowest spacing where present value is maximized by flowing at the maximum possible rate. Practically, it may be advantageous to use a smaller spacing because this may reduce fracturing costs and increase the probability of establishing a good connection between the wellbores.

As long as the present value is optimized by flowing at the maximum possible rate through the system, it is advantageous to increase fracture transmissivity (for example, by using proppant).

For design of an actual multiple stage EGS doublet, a more sophisticated physical model and optimization scheme would be needed. In addition, the optimization would need to consider marginal cost, not only marginal revenue. A final decision on whether to attempt a commercial EGS project would require consideration of all costs associated with the project over the lifetime of the system. Because make-up wells could be drilled, EGS wells could be designed to thermally decline at a timescale shorter than the life span of the power plant.

The calculations show that a lateral length of 1000 m is sufficient to access an adequate volume of rock for wells with spacing of 400 m or more. For closer well spacing, even longer laterals may be preferred.

The sensitivity analysis demonstrates that multiple stage fracturing designs radically improve EGS economic performance. Developing and testing technology that enables multiple stage fracturing and horizontal drilling for EGS needs to be a high priority for future research and development.

Acknowledgements

Thank you to the Cockrell School of Engineering at the University of Texas at Austin for supporting this research. Thank you very much to Thomas Doe for his thoughtful comments and also for sharing his code for implementing the Gringarten et al. (1975) finite fracture spacing calculation. We appreciate the detailed and constructive feedback from two anonymous reviewers.

References

Baria, R., Michelet, S., Baumgärtner, J., Dyer, B., Gerard, A., Nicholls, J., Hettkamp, T., Teza, D., Soma, N., Asanuma, H., Garnish, J., Megel, T., 2004. Microseismic monitoring of the world's largest potential HDR reservoir. Paper Presented at the Twenty-Ninth Workshop on Geothermal Reservoir Engineering, Stanford University.

Barton, N., Bandis, S., Bakhtar, K., 1985. Strength, deformation and conductivity coupling of rock joints. Int. J. Rock Mech. Min. Sci. Geomech. Abstr. 22 (3), 121–140, http://dx.doi.org/10.1016/0148-9062(85)93227-9.

Becker, M.W., Cole, M., Ciervo, C., 2016. Measuring hydraulic connection in fractured bedrock with periodic hydraulic tests and distributed acoustic sensing. Paper Presented at the 41st Workshop on Geothermal Reservoir Engineering, Stanford University.

Bendall, B., Hogarth, R., Holl, H., McMahon, A., Larking, A., Reid, P., 2014. Australian experiences in EGS permeability enhancement – a review of 3 case studies. Paper Presented at the Thirty-Ninth Workshop on Geothermal Reservoir Engineering, Stanford University.

Brown, D.W., Duchane, D.V., Heiken, G., Hriscu, V.T., 2012. Mining the Earth's Heat: Hot Dry Rock Geothermal Energy. Springer-Verlag.

Chen, N.H., 1979. An explicit equation for friction factor in pipe. Ind. Eng. Chem. Fundam. 18 (3), 296–297.

Cipolla, C., Warpinski, N., Mayerhofer, M., Lolon, E., Vincent, M., 2008. The relationship between fracture complexity, reservoir properties, and fracture treatment design. Paper Presented at the SPE Annual Technical Conference and Exhibition , Denver, Colorado, USA.

Cremer, G.M., Duffield, R.B., Nunz, G.J., Smith, M.C., Wilson, M.G., 1980. Hot Dry Rock Geothermal Energy Development Program Annual Report, Los Alamos National Lab.

Dezayes, C., Genter, A., Valley, B., 2010. Structure of the low permeable naturally fractured geothermal reservoir at Soultz. C.R. Geosci. 342 (7–8), 517–530, http://dx.doi.org/10.1016/j.crte.2009.10.002.

Doe, T., McLaren, R., 2016. Discrete fracture network analysis of controlling factors for EGS performance. Paper Presented at the 41st Workshop on Geothermal Reservoir Engineering, Stanford University.

Doe, T., McLaren, R., Dershowitz, W., 2014. Discrete fracture network simulations of enhanced geothermal systems. Paper Presented at the Thirty-Ninth Workshop on Geothermal Reservoir Engineering, Stanford University.

Evans, K.F., 2005. Permeability creation and damage due to massive fluid injections into granite at 3.5 km at Soultz: 2. Critical stress and fracture strength. J. Geophys. Res. 110 (B4), http://dx.doi.org/10.1029/2004JB003169.

Fox, D.B., Sutter, D., Beckers, K.F., Lukawski, M.Z., Koch, D.L., Anderson, B.J., Tester, J.W., 2013. Sustainable heat farming: modeling extraction and recovery in discretely fractured geothermal reservoirs. Geothermics 46, 42–54, http://dx.doi.org/10.1016/j.geothermics.2012.09.001.

Genter, A., Evans, K., Cuenot, N., Fritsch, D., Sanjuan, B., 2010. Contribution of the exploration of deep crystalline fractured reservoir of Soultz to the knowledge of enhanced geothermal systems (EGS). C.R. Geosci. 342 (7–8), 502–516, http://dx.doi.org/10.1016/j.crte.2010.01.006.

Glauser, W., McLennan, J., Walton, I., 2013. Do perforated completions have value for engineered geothermal systems. In: Bunger, A., McLennon, J., Jeffrey, R. (Eds.), Effective and Sustainable Hydraulic Fracturing. InTech.

Green, A.S.P., Parker, R.H., 1992. A multi-cell design of a HDR reservoir. Geothermal Resources Council Transactions 16.

Gringarten, A.C., Witherspoon, P.A., Ohnishi, Y., 1975. Theory of heat extraction from fractured hot dry rock. J. Geophys. Res. 80 (8), 1120–1124, http://dx.doi.org/10.1029/JB080i008p01120.

Hasan, A.R., Kabir, C.S., 2002. Fluid Flow and Heat Transfer in Wellbores. Society of Petroleum Engineers, Richardson, TX.

Ito, H., Kaieda, H., 2002. Review of 15 years experience of the Ogachi hot dry rock project with emphasis on geological features. Paper Presented at the 24th New Zealand Geothermal Workshop.

Jung, R., 1989. Hydraulic in situ investigations of an artificial fracture in the Falkenberg granite. Int. Journal of Rock Mech. Min. Sci. Geomech. Abstr. 26 (3–4), 301–308, http://dx.doi.org/10.1016/0148-9062(89)91978-5.

Jung, R., 2013. EGS – goodbye or back to the future. In: Andrew, P.B., McLennan, J., Jeffrey, R. (Eds.), Effective and Sustainable Hydraulic Fracturing. InTech., pp. 95–121.

King, G., 2010. Thirty years of gas shale fracturing: what have we learned? Paper Presented at the SPE Annual Technical Conference and Exhibition, Florence.

Lecampion, B., Desroches, J., Weng, X., Burghardt, J., Brown, J.E., 2015. Can we engineer better multistage horizontal completions? Evidence of the importance of near-wellbore fracture geometry from theory, lab, and field experiments. Paper Presented at the SPE Hydraulic Fracturing Technology Conference, The Woodlands, TX, http://dx.doi.org/10.2118/173363-MS, SPE-173363-MS.

Li, T., Shiozawa, S., McClure, M., 2014. Thermal breakthrough calculations to optimize design of a multiple-stage enhanced geothermal system. Geotherm. Res. Council Trans., 38.

Lowry, T.S., Kalinina, E.A., Hadgu, T., Klise, K.A., Malczynski, L.A., 2014. Economic valuation of directional wells for EGS heat extraction. Paper Presented at the Thirty-Ninth Workshop on Geothermal Reservoir Engineering, Stanford University.
MacDonald, P., Stedman, A., Symons, G., 1992. The UK geothermal hot dry rock R&D programme. Paper Presented at the Seventeenth Workshop on Geothermal Reservoir Engineering, Stanford University.
McClure, M., 2009. Fracture stimulation in enhanced geothermal systems. MS Thesis. Stanford University.
McClure, M.W., Horne, R.N., 2014. An investigation of stimulation mechanism in enhanced geothermal systems. Int. J. Rock Mech. Min. Sci. 72, 242–260, http://dx.doi.org/10.1016/j.ijrmms.2014.07.011.
Mégel, T., Kohl, T., Gérard, A., Rybach, L., Hopkirk, R., 2005. Downhole pressures derived from wellhead measurements during hydraulic experiments. Paper Presented at the World Geothermal Congress, Antalya, Turkey.
Mines, G., Nathwani, J., 2013. Estimated power generation costs for EGS. Paper Presented at the Thirty-Eighth Workshop on Geothermal Reservoir Engineering, Stanford University.
Miyairi, M., Sorimachi, M., 1996. Characterization of effective fractures by production logging at Hijiori HDR test site. Paper Presented at the Second Well Logging Symposium of Japan, Makuhari, Japan.
Murphy, H.D., Fehler, M.C., 1986. Hydraulic fracturing of jointed formations. Paper Presented at the International Meeting on Petroleum Engineering, Beijing, China, SPE-14088-MS http://dx.doi.org/10.2118/14088-MS.
Ogoke, V.C., Schauerte, L.J., Bouchard, G., Inglehart, S.C., 2014. Simultaneous operations in multi-well pad: a cost effective way of drilling multi wells pad and deliver 8 fracs a day. Paper Presented at the SPE Annual Technical Conference and Exhibition, Amsterdam, The Netherlands, SPE-170744-MS http://dx.doi.org/10.2118/170744-MS.
Olson, J., Augustine, C., Eustes, A., Fleckenstein, W., 2015. Design considerations for applying multi-zonal isolation techniques in horizontal wells in a geothermal setting. Paper presented at the Fortieth Workshop on Geothermal Reservoir Engineering. Stanford University.
Parker, R., 1999. The Rosemanowes HDR project 1983–1991. Geothermics 28 (4–5), 603–615, http://dx.doi.org/10.1016/S0375-6505(99)00031-0.
Petty, S., Nordin, Y., Glassley, W., Cladouhos, T.T., Swyer, M., 2013. Improving geothermal project economics with multi-zone stimulation: results from the Newberry Volcano EGS demonstration. Paper Presented at the Thirty-Eighth Workshop on Geothermal Reservoir Engineering, Stanford, CA.
Pine, R.J., Batchelor, A.S., 1984. Downward migration of shearing in jointed rock during hydraulic injections. Int. J. Rock Mech. Min. Sci. Geomech. Abstr. 21 (5), 249–263, http://dx.doi.org/10.1016/0148-9062(84)92681-0.
Richards, H.G., Parker, R.H., Green, A.S.P., Jones, R.H., Nicholls, J.D.M., Nicol, D.A.C., Randall, M.M., Richards, S., Stewart, R.C., Willis-Richards, J., 1994. The performance and characteristics of the experimental hot dry rock geothermal reservoir at Rosemanowes, Cornwall (1985–1988). Geothermics 23 (2), 73–109, http://dx.doi.org/10.1016/0375-6505(94)90032-9.
Sanyal, S.K., 2010. On minimizing the levelized cost of electric power from enhanced geothermal systems. Paper Presented at the World Geothermal Congress, Bali, Indonesia.
Sanyal, S.K., Butler, S.J., 2005. An analysis of power generation prospects from enhanced geothermal systems. GRC Trans. 29, 131–138.
Serpen, U., Aksoy, N., 2015. Successful perforation operation experience in a geothermal well of Salavatli geothermal field. Paper Presented at the Fourtieth Workshop on Geothermal Reservoir Engineering, Stanford University.
Shear, T., 2015. Whole Sale Power Prices Increase Across the Country in 2014. U. S. Energy Information Administration.
Shiozawa, S., McClure, M., 2014. EGS designs with horizontal wells, multiple stages, and proppant. Paper Presented at the Thirty-Ninth Workshop on Geothermal Reservoir Engineering, Stanford, CA.
Tenma, N., Yamaguchi, T., Zyvoloski, G., 2008. The Hijiori hot dry rock test site, Japan evaluation and optimization of heat extraction from a two-layered reservoir. Geothermics 37, 19–52, http://dx.doi.org/10.1016/j.geothermics.2007.11.002.
Tester, J. (Ed.), 2006. The Future of Geothermal Energy: Impact of Enhanced Geothermal Systems (EGS) on the United States in the 21st Century. Massachusetts Institute of Technology.
Tischner, T., Pfender, M., Teza, D., 2006. Hot Dry Rock Projekt Soultz: Erste Phase Der Erstellung Einer Wissenschaftlichen Pilotanlage: Final Project Report. Bundesanstalt für Geowissenschaften und Rohstoffe (BGR).
Tischner, T., Schindler, M., Jung, R., Nami, P., 2007. HDR project Soultz: hydraulic and seismic observations during stimulation of the 3 deep wells by massive water injections. Paper Presented at the Thirty-Second Workshop on Geothermal Reservoir Engineering, Stanford University, Stanford, CA.
Wang, Z., McClure, M.W., Horne, R.N., 2009. A single-well EGS configuration using a thermosiphon. Paper Presented at the Thirty-Fourth Workshop on Geothermal Reservoir Engineering, Stanford University, Stanford, CA.
Willingham, J.D., Tan, H.C., Norman, L.R., 1993. Perforation friction pressure of fracturing fluid slurries. Paper presented at the SPE Rocky Mountain Regional/Low Permeability Reservoirs Symposium, Denver, CO, SPE 25891.
Wyborn, D., de Graaf, L., Davidson, S., Hann, S., 2005. Development of Australia's first hot fractured rock (HFR) underground heat exchanger, Cooper Basin, South Australia. Paper Presented at the World Geothermal Congress, Antalya, Turkey, 24–29 April 2005.
Yoshioka, K., Jermia, J., Pasikki, R., Ashadi, A., 2015. Zonal hydraulic stimulation in the Salak geothermal field. Paper Presented at the World Geothermal Congress, Melbourne, Australia.
Zimmermann, G., Reinicke, A., Blöcher, G., Moeck, I., Kwiatek, G., Brandt, W., Regenspurg, S., Schulte, T., Saadat, A., Huenges, E., 2010. Multiple fracture stimulation treatments to develop an enhanced geothermal system (EGS) – conceptual design and experimental results. Paper Presented at the Word Geothermal Congress, Bali, Indonesia.